J|A|C|S
ARTICLES
Published on Web 09/20/2003

Nonenzymatic Breakdown of the Tetrahedral (α-Carboxyketal Phosphate) Intermediates of MurA and AroA, Two Carboxyvinyl Transferases. Protonation of Different Functional Groups Controls the Rate and Fate of Breakdown

Bartosz Byczynski,[†,§] Shehadeh Mizyed,[†,§] and Paul J. Berti*[,†,‡,§]

Contribution from the Department of Chemistry, Department of Biochemistry, and Antimicrobial Research Centre, McMaster University, 1280 Main Street West, Hamilton, ON, L8S 4M1, Canada

Received March 3, 2003; E-mail: berti@mcmaster.ca

Abstract: The mechanisms of nonenzymatic breakdown of the tetrahedral intermediates (THIs) of the carboxyvinyl transferases MurA and AroA were examined in order to illuminate the interplay between the inherent reactivities of the THIs and the enzymatic strategies used to promote catalysis. THI degradation was through phosphate departure, with C−O bond cleavage. It was acid catalyzed and dependent on the protonation state of the carboxyl of the α-carboxyketal phosphate functionality, with ionizations at pK_a = 3.2 ± 0.1 and 4.3 ± 0.1 for MurA and AroA THIs, respectively. The solvent deuterium kinetic isotope effect for MurA THI at pL 2.0 was 1.3 ± 0.4, consistent with general acid catalysis. The pK_a's suggested intramolecular general acid catalysis through protonation of the bridging oxygen of the phosphate, though H_3O^+ catalysis was also possible. The product distribution varied with pH. The dominant breakdown products were {pyruvate + phosphate + R−OH} (R−OH = UDP-GlcNAc or shikimate 3-phosphate) at all pH's, particularly low pH. At higher pH's, increasing proportions of ketal, arising from intramolecular substitution of phosphate by the adjacent hydroxyl and the *enol*pyruvyl products of phosphate elimination were observed. With MurA THI, the product distribution fitted to pK_a's 1.6 and 6.2, corresponding to the expected pK_a's of a phosphate monoester. C−O bond cleavage was demonstrated by the lack of monomethyl [^{33}P]phosphate formed upon degrading MurA [^{33}P]THI in 50% methanol. General acid catalysis through the bridging oxygen is consistent with the location of the previously proposed general acid catalyst for THI breakdown in AroA, Lys22.

The mechanisms of enzymatic reactions reflect an interplay between the inherent reactivities of the substrate(s) and whatever catalytic strategies may be employed to lower activation energies. To understand enzyme mechanisms, we must therefore also understand the analogous nonenzymatic reactions to learn which catalytic strategies will be effective and which will not.

The enzymes MurA[1−6] and AroA (EPSP synthase)[7−10] have been extensively studied because of their novel catalytic mechanisms and because they are targets for biocidal agents.[11,12] They are the only two enzymes known to catalyze carboxyvinyl transfer with phospho*enol*pyruvate (PEP). Both enzymes catalyze their reactions through fully reversible addition/elimination mechanisms that pass through tetrahedral intermediates (THIs, Figure 1).

Relatively little is known about the stability and reactivity of the THIs; they appear to be the only examples in the chemical literature of acyclic α-carboxyketal phosphates. Two compounds with related functionalities are CMP-NeuAc (**1**) and CMP-deoxyoctonate (**2**), which possess α-carboxyketal phosphodiester groups.

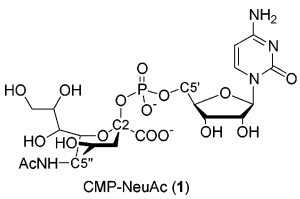

CMP-NeuAc (**1**)

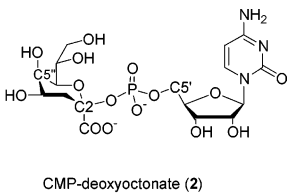

CMP-deoxyoctonate (**2**)

THIs are unstable, especially at low pH. MurA THI was reported to have half-lives of 38 s at pH 5 and 2 h at pH 8,[13] while AroA THI half-lives were 45 min at pH 7 and >48 h at

[†] Department of Chemistry.
[‡] Department of Biochemistry.
[§] Antimicrobial Research Centre.

(1) Abbreviations: AroA, EPSP synthase; $AroA_{H6}$, AroA with a C-terminal extension terminating with His_6; CMP, cytidine 5′-monophosphate; CMP-NeuAc, cytidine 5′-monophosphate *N*-acetyl neuraminic acid; EPSP, *enol*pyruvylshikimate 3-phosphate; EP-UDP-GlcNAc, *enol*pyruvyl uridine diphospho *N*-acetyl-glucosamine; KIE, kinetic isotope effect; MurA, EP-UDP-GlcNAc synthase; HMBC, heteronuclear multiple bond correlation spectroscopy; NeuAc, *N*-acetyl neuraminic acid; PEP, phospho*enol*pyruvate; Pi, inorganic phosphate; PMSF, phenylmethylsulfonyl fluoride; S3P, shikimate 3-phosphate; THI, tetrahedral intermediate; UDP-GlcNAc, uridine diphospho *N*-acetylglucosamine.

(2) Gunetileke, K. G.; Anwar, R. A. *J. Biol. Chem.* **1968**, *243*, 5770.
(3) Marquardt, J. L.; Siegele, D. A.; Kolter, R.; Walsh, C. T. *J. Bacteriol.* **1992**, *174*, 5748.
(4) Marquardt, J. L.; Brown, E. D.; Walsh, C. T.; Anderson, K. S. *J. Am. Chem. Soc.* **1993**, *115*, 10398.
(5) Lees, W. J.; Walsh, C. T. *J. Am. Chem. Soc.* **1995**, *117*, 7329.
(6) Schonbrunn, E.; Sack, S.; Eschenburg, S.; Perrakis, A.; Krekel, F.; Amrhein, N.; Mandelkow, E. *Structure* **1996**, *4*, 1065.
(7) Anderson, K. S.; Johnson, K. A. *Chem. Rev.* **1990**, *90*, 1131.

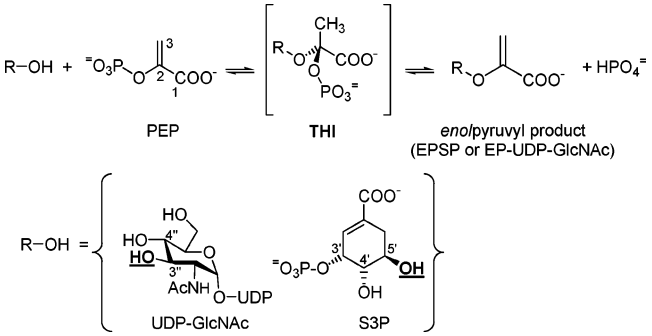

Figure 1. Reactions catalyzed by the carboxyvinyl transferases MurA and AroA. R−OH is uridine 5′-diphospho *N*-acetylglucosamine (UDP-GlcNAc) for MurA and shikimate 3-phosphate (S3P) for AroA. The reactive hydroxyls are underlined.

pH 12.[14] At pH 4, the products were S3P, pyruvate, and phosphate (Pi) (**3**). At pH 7 the products also included *enol*pyruvyl S3P (EPSP, **5**) and the ketal (**4**) formed by substitution of the phosphate with S3P O4′H.

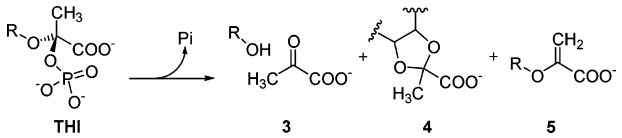

AroA accelerates THI breakdown by $>10^6$-fold in order to achieve the observed rates of catalytic turnover.[14] The mechanistic imperative of the enzymes is thus 2-fold, to promote THI breakdown and at the same time to form the correct *enol*pyruvyl products, not {R−OH[15] + pyruvate + Pi}. The acid lability of the THIs implies that acid catalysis promotes phosphate and/or R−OH departure. However, important questions remain, including the following: (i) what atom or functional group is protonated to promote breakdown; (ii) how effective can acid catalysis be; that is, how much can it accelerate the reaction; (iii) how does this compare with the catalytic enhancement attributed to the general acid catalyst in the AroA-catalyzed reaction; and (iv) what controls the product distribution? Answering these questions will help answer the question of how AroA and MurA accelerate and control THI breakdown.

Studies on the THIs have been limited by the difficulty in making them. They are obtained in substoichiometric amounts by quenching enzymatic reactions in KOH, yielding 50−200 nmol of THI per synthesis. By producing gram amounts of *E. coli* AroA and MurA and using them to synthesize THIs, we have been able to characterize the kinetics and products of THI breakdown over a pH range of 1−12.

Materials and Methods

General. [1-^{14}C]PEP and [$^{13}C_3$]PEP were prepared from labeled pyruvates (Amersham Biosciences and Cambridge Isotope Laboratories, respectively) using pyruvate phosphate dikinase[16] (a generous gift from Prof. D. Dunaway-Mariano, University of New Mexico) as described previously.[17] [^{33}P]PEP was prepared from [γ-^{33}P]ATP essentially as described previously.[18] The AroA ketal product was prepared as described previously[19] and purified under the same conditions as AroA THI (see below).

Enzymes. Recombinant *E. coli* AroA bearing a C-terminal His_6 tag to allow Ni^{2+}-affinity purification, $AroA_{H6}$, was prepared as described previously.[17]

Recombinant *E. coli* MurA was PCR amplified from *E. coli* strain DH5α and ligated into the pET41a plasmid (Novagen, Inc.), replacing the *NdeI*−*BamHI* fragment. The insert was sequenced and found to have the same amino acid sequence as that of Genbank entry P28909. The MurA-containing plasmid was transformed into *E. coli* strain BL21*(DE3) (Invitrogen).

LB broth containing 30 μg/mL kanamycin was inoculated with 1 vol % of overnight culture and grown at 37 °C until $OD_{600} = 0.6$. MurA expression was induced with 1mM isopropyl-β-D-thiogalactopyranoside (IPTG) for 4 h at 37 °C. The cells were harvested by centrifugation at 5000 × *g* for 10 min, and the pellet was resuspended in 10 mL per L of culture of buffer A (50 mM Tris·HCl, pH 7.5, 1 mM EDTA, 1 mM phenylmethylsulfonyl fluoride (PMSF), 1 mM benzamidine) and frozen or lysed immediately.

All subsequent steps were performed at 0−4 °C. DNase and RNase (100μg/mL) were added to the resuspended cells immediately before lysis in a French press. Cell debris was removed by centrifugation at 10 000 × *g* for 10 min. The protein was precipitated in 70% saturated ammonium sulfate and pelleted by centrifugation at 20 000 × *g* for 10 min, followed by resuspension in buffer A + 1 M ammonium sulfate. Insoluble material was removed by centrifugation at 20 000 × *g* for 10 min. MurA was purified by hydrophobic interaction chromatography on a 40 mL Phenyl Sepharose (high sub, Amersham Biosciences) column, with elution on a gradient of 1−0 M ammonium sulfate in buffer A over five column volumes at a 5 mL/min flow rate with A_{280} detection. MurA eluted at near 0.5 M ammonium sulfate. The buffer was exchanged by diafiltration over a YM-10 (Amicon) membrane to buffer A. It was further purified by anion exchange chromatography on a 40 mL Q-Sepharose (fast flow, Amersham Biosciences) column. MurA was eluted on a gradient of 0−1 M KCl in buffer A. MurA was the first of two peaks eluted, near 0.2 M KCl. It was concentrated over a YM-10 membrane to a concentration of 1−3 mM (50−150 mg/mL). The protein concentration was determined from the A_{280}, using $\epsilon_{280} = 13\,250\ M^{-1}\ cm^{-1}$, as determined by the method of Edelhoch.[20] Aliquots were flash frozen in liquid nitrogen and stored at −80 °C. Yields were typically 40−75 mg/L of culture.

THI Synthesis: MurA. Reaction mixtures (up to 2000 μL) containing 2 mM MurA, 2 mM UDP-GlcNAc, 200 μM PEP, and 50 mM potassium phosphate, pH 7.5, were prepared and quenched after 5 s with KOH to 200 mM. The quenched reaction was extracted repeatedly with chloroform to precipitate and remove all protein. THI was purified on a Mono-Q anion exchange column (5 × 50 mm^2, Amersham Biosciences) with a gradient of 100−500 mM KCl in 10 mM NH_4Cl, pH 10 over 15 column volumes at a 0.5 mL/min flow rate and A_{260} detection. MurA [^{14}C]THI synthesis was as above but with 0.5 μCi [1-^{14}C]PEP. In some reactions, MurA THI was purified by anion exchange chromatography using ammonium bicarbonate, pH 10

(8) Anderson, K. S.; Sammons, R. D.; Leo, G. C.; Sikorski, J. A.; Benesi, A. J.; Johnson, K. A. *Biochemistry* **1990**, *29*, 1460.
(9) Anderson, K. S.; Sikorski, J. A.; Johnson, K. A. *Biochemistry* **1988**, *27*, 1604.
(10) Anderson, K. S.; Sikorski, J. A.; Johnson, K. A. *Biochemistry* **1988**, *27*, 7395.
(11) Hendlin, D.; Stapley, E. O.; Jackson, M.; Wallick, H.; Miller, A. K.; Wolf, F. J.; Miller, T. W.; Chaiet, L.; Kahan, F. M.; Foltz, E. L.; Woodruff, H. B.; Mata, J. M.; Hernandez, S.; Mochales, S. *Science* **1969**, *166*, 122.
(12) Sikorski, J. A.; Gruys, K. J. *Acc. Chem. Res.* **1997**, *30*, 2.
(13) Kim, D. H.; Lees, W. J.; Haley, T. M.; Walsh, C. T. *J. Am. Chem. Soc.* **1995**, *117*, 1494.
(14) Anderson, K. S.; Johnson, K. A. *J. Biol. Chem.* **1990**, *265*, 5567.
(15) R−OH refers to both the O3″H of UDP-GlcNAc and O5′H of S3P (Figure 1).
(16) Wang, H. C.; Ciskanik, L.; Dunaway-Mariano, D.; von der Saal, W.; Villafranca, J. J. *Biochemistry* **1988**, *27*, 625.
(17) Mizyed, S.; Wright, J. E. I.; Byczynski, B.; Berti, P. J. *Biochemistry* **2003**, *42*, 6986.
(18) Roossien, F. F.; Brink, J.; Robillard, G. T. *Biochim. Biophys. Acta* **1983**, *760*, 185.
(19) Leo, G. C.; Sikorski, J. A.; Sammons, R. D. *J. Am. Chem. Soc.* **1990**, *112*, 1653.
(20) Pace, C. N.; Vajdos, F.; Fee, L.; Grimsley, G.; Gray, T. *Protein Sci.* **1995**, *4*, 2411.

in the gradient instead of KCl. The yield of MurA THI was 3−10% relative to the protein concentration, with a specific activity of ∼1.2 mCi/mmol in [^{14}C]THI.

THI Synthesis: AroA. AroA THI was prepared as described previously.[17] Briefly, the quenching method was similar to MurA reactions, but KOH and KOH-saturated 2-propanol were needed to denature the protein. Anion exchange chromatography used a gradient of triethylammonium chloride ($Et_3NH{\cdot}Cl$). Triethylammonium salts were required to resolve THI from EPSP.[14,17] The yield of AroA THI was 2.5−5% relative protein concentration.

THI Breakdown. The rate and product distribution of THI breakdown were quantitated using HPLC separation under similar conditions to those above, with quantitation of products and residual THI by A_{260} (MurA THI only) or ^{14}C (AroA and MurA THI). All THI breakdown experiments were conducted at 25 °C.

Purified MurA THI contained ca. 300 mM KCl from the chromatography buffer, with a minimal amount of NH_4Cl (10 mM) to control pH. For breakdown reactions, the purified THI (50 μL, ∼1.5 nmol) was diluted with 450 μL of buffer (50 mM final concentration) at the desired pH. The buffers used were as follows: pH < 2, HCl; pH 2.5−3.5, glycine; pH 4.0−5.5, acetate; pH 6.0−9.5, bis(trispropane); pH 7.5−8.5, Tris; pH 9.5−0.5, glycine; pH 12, KOH. Chromatographic conditions were as those for THI synthesis but with a flow rate of 1.0 mL/min. If necessary, reactions were stopped with KOH to pH 12 before HPLC injection. For reactions at pH > 9, KOH traps were used to prevent atmospheric CO_2 from entering the solution and lowering the pH. Without KOH traps, THIs appeared to be stable for several days and then quickly degraded as the pH dropped.

The solvent deuterium kinetic isotope effect (KIE) was measured at pL 2.0 using 50 μL of MurA THI prepared as described above and 450 μL of buffer containing >99% with D_2O, with the pL adjusted with concentrated HCl. The pH meter reading was adjusted by 0.4 units: pL = pH(meter reading) + 0.4.[21] The solvent deuterium molar fraction was thus 0.90, and the observed reaction rate was extrapolated to a deuterium molar fraction of 1.0.

Purified AroA THI contained ca. 700 mM $Et_3NH{\cdot}Cl$, pH 9.0 from the chromatography buffer. In a typical reaction, 100 μL of THI (ca. 1000 cpm ^{14}C) was mixed with 750 μL of buffer (50 mM final concentration), which gave ca. 100 mM of $Et_3NH{\cdot}Cl$ in the reaction mixture. The added buffer had a higher or lower pH than the target pH to compensate for the buffering capacity of $Et_3NH{\cdot}Cl$. The pH was determined using test mixtures containing the same buffer composition as those the reaction mixtures. The reaction buffers used were as follows: pH < 4, glycine; pH 4−6, citrate; pH 6−8, Tris; pH 8−9, bis(trispropane); pH > 9.0, triethylamine. If necessary, reactions were stopped with KOH to pH 12 before HPLC injection.

MurA [^{33}P]THI Breakdown in Methanol. MurA [^{33}P]THI was reacted in 50% (v/v) methanol to determine whether there was P−O bond cleavage. Reaction conditions were as those above except for the inclusion of methanol. The products were separated on a Mono-Q column with a gradient of 20−500 mM KCl in 10 mM KOH, pH 12, over 15 column volumes at a flow rate of 0.5 mL/min. Because the products could not be detected by absorbance, reaction mixtures were spiked with 5 μmol of monomethyl phosphate and 0.5 μmol of phosphate immediately before chromatography. Fractions were collected, and the Malachite Green assay was used to detect phosphate.[22] Monomethyl phosphate did not react directly with Malachite Green and was first treated with alkaline phosphatase (Sigma) to release phosphate. This made it possible to distinguish between the two products. Monomethyl phosphate and phosphate eluted at 4.5 and 8.0 min, respectively.

NMR of MurA Ketal (4). The ketal product (17 μg) of MurA [$^{13}C_3$]-THI breakdown at pH 7.5 was repurified and identified by NMR. One-dimensional ^{1}H, ^{13}C, and two-dimensional HMBC spectra were collected using a 5 mm inverse geometry probe at 600 MHz for ^{1}H. The HMBC spectrum was collected in 128 increments with 256 scans per increment and a delay time of 1 s between scans. The data were linear-predicted in F_1 to 1024 points before Fourier transformation. The spectra were collected without ^{13}C decoupling, so correlations are seen to the ^{13}C satellites of the methyl signal in the ^{1}H spectrum.

Data Analysis. pK_a values for rates and product distributions were fitted by nonlinear regression to equations for single or double ionizations (eqs 1 and 2), with proportional weighting of data points, using the program Grafit (Erithacus Software Ltd.).

$$y = \frac{\text{Limit}_1 + \text{Limit}_3 \times 10^{(\text{p}H-\text{p}K_j)}}{10^{(\text{p}H-\text{p}K_j)} + 1} \quad (1)$$

$$y = \frac{\text{Limit}_1 + \text{Limit}_2 \times 10^{(\text{p}H-\text{p}K_j)}}{10^{(\text{p}H-\text{p}K_j)} + 1} - \frac{(\text{Limit}_2 - \text{Limit}_3) \times 10^{(\text{p}H-\text{p}K_k)}}{10^{(\text{p}H-\text{p}K_k)} + 1} \quad (2)$$

For k-versus-pH profiles, $y = k_i$, the rate constant at pH = i; Limit$_1$ to Limit$_3$ were k_{max}, k_{mid}, and k_{min} at low, mid, and high pH, respectively; and pK_j = pK_{a2}, pK_k = pK_{a4}. For product-versus-pH profiles, $y = f(X)_i$, the fraction of product X formed at pH = i, Limit$_1$ to Limit$_3$ were $f(X)_{low}$, $f(X)_{mid}$, and $f(X)_{high}$ at low, mid, and high pH, respectively, and pK_j = pK_{a1}, pK_k = pK_{a3}. The fraction of products were calculated as for example, $f(\mathbf{3}) = [\mathbf{3}]/([\mathbf{3}] + [\mathbf{4}] + [\mathbf{5}])$, and so forth.

For AroA THI, an alternate method of was used for fitting the k-versus-pH data. Fitting directly to eq 1 gave a curve that was visibly below most of the data points (data not shown).[23] A better fit was achieved by a linear fit of log(k)-versus-pH and setting k_{max} to the average of k at the lowest pH values. The value of k_{min} was estimated by then fitting to eq 1 with k_{max} and pK_a fixed. For some fitted curves for product distributions, the limits at extrema were fixed; that is, $f(\mathbf{3})_{low} = 1.0$, $f(\mathbf{4})_{low} = 0$, and $f(\mathbf{5})_{low} = 0$. Fixing these values in the fitted curves gave greater consistency in pK_a's. When not fixed, the fitted values of $f(X)_{low}$ were within 0.004 of the fixed values.

Results

The rate constants and product distribution of THI breakdown were determined for both the MurA and AroA THIs (Table 1, Figures 2 and 3). It was possible to follow MurA THI breakdown by anion exchange HPLC using absorbance detection of the uracil ring at 260 nm or detection of the labeled products of [1-^{14}C]THI breakdown. Detection of AroA THI breakdown was by ^{14}C only as it is a poor chromophore and the anion exchange buffer, triethylammonium chloride,[14,17] had significant UV absorbance. MurA THI breakdown was shown by UV absorbance detection to follow first-order kinetics at all pH's (data not shown). AroA THI breakdown was also therefore assumed to follow first-order kinetics, making it possible to determine rates at a given pH with one or a few time points.

Breakdown Rates. The pH dependence of the MurA THI breakdown rate was most consistent with two ionizations, the most important one with pK_{a2} = 3.2 ± 0.1 and a second ionization with pK_{a4} = 8.8 ± 0.3. The AroA data were fitted to

(21) Salomaa, P.; Schaleger, L. L.; Long, F. A. *J. Am. Chem. Soc.* **1964**, *86*, 1.
(22) Lanzetta, P. A.; Alvarez, L. J.; Reinach, P. S.; Candia, O. A. *Anal. Biochem.* **1979**, *100*, 95.

(23) This was an artifact arising from fitting relatively noisy data to a logarithm-containing equation. With proportional weighting, deviation of the fitted curve below the data points is less unfavorable than deviation above the data points, and therefore the fitted curve is below most of the data points. The effect can be observed by graphing simulated data on a log scale with error bars equal to >50% of each point. For experimental data with small errors, such as with MurA THI, this effect is negligible. The parameters derived from fitting directly to eq 1 were pK_a = 4.0, $k_{max} = 0.66\ s^{-1}$, $k_{min} = 3 \times 10^{-7}\ s^{-1}$. The differences from the values in Table 1 were chemically insignificant.

Table 1. pH Dependence of Rate Constants and Product Distributions

		MurA THI	AroA THI
	rate constants		
	pK_{a2}	3.2 ± 0.1	4.3 ± 0.1
	pK_{a4}	8.8 ± 0.3	
	k_{max} (s^{-1})	0.72 ± 0.12	0.79 ± 0.08
	k_{mid} (s^{-1})	$(1.6 \pm 0.8) \times 10^{-5}$	
	k_{min} (s^{-1})	$(7 \pm 3) \times 10^{-8}$ [a]	$(3 \pm 3) \times 10^{-7}$ [a]
	product distribution		
{R−OH + pyruvate + Pi} (**3**)	pK_{a1}	1.7 ± 0.3	
	pK_{a3}	6.2 ± 0.1	4.7 ± 0.4
	$f(\mathbf{3})_{low}$	1 [b]	
	$f(\mathbf{3})_{mid}$	0.986 ± 0.001	0.94 ± 0.03
	$f(\mathbf{3})_{high}$	0.907 ± 0.002	0.66 ± 0.03
{ketal + Pi} (**4**)	pK_{a1}	1.5 ± 0.1	
	pK_{a3}	6.1 ± 0.1	6.0 ± 0.6
	$f(\mathbf{4})_{low}$	0 [b]	
	$f(\mathbf{4})_{mid}$	0.012 ± 0.001	0.02 ± 0.01
	$f(\mathbf{4})_{high}$	0.062 ± 0.003	0.12 ± 0.02
{*enol*pyruvyl + Pi} (**5**)	pK_{a1}		
	pK_{a3}	6.2 ± 0.2	4.5 ± 0.7
	$f(\mathbf{5})_{low}$		
	$f(\mathbf{5})_{mid}$	0 [b]	0.05 ± 0.04
	$f(\mathbf{5})_{high}$	0.030 ± 0.006	0.23 ± 0.03

[a] The numerical value of k_{min} was almost completely defined by single k_i at the highest pH measured. [b] Value fixed in fitted curves.

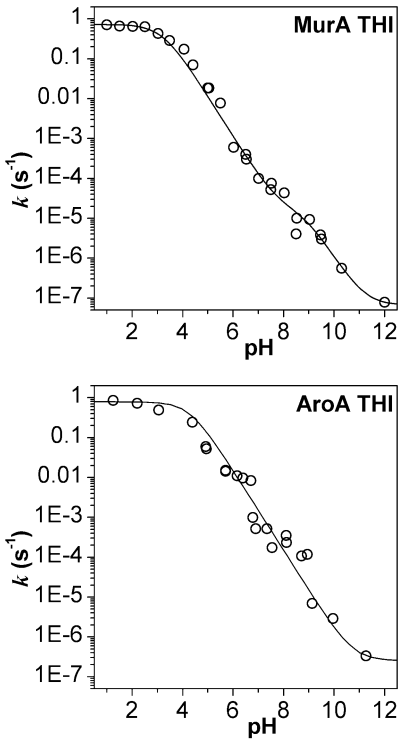

Figure 2. Rate constant profiles of THI breakdown for (top) MurA THI and (bottom) AroA THI. Solid lines represent fitted curves.

a single ionization, $pK_{a2} = 4.3 \pm 0.1$. The solvent deuterium KIE for MurA THI breakdown at pL 2.0 was 1.3 ± 0.4.

Breakdown Products: MurA THI. The MurA THI structure was determined previously;[4] in the present study, MurA [$^{13}C_3$]-THI was synthesized and its identity confirmed by ^{13}C NMR (data not shown). Repurification and ^{13}C NMR of 17 μg of the putative ketal (**4**, Figure 4) and *enol*pyruvyl (**5**, data not shown) products confirmed their structures. The ketal (**4**) has not been characterized previously. The ^1H NMR spectrum was not informative because the sample contained some contaminating UDP-GlcNAc. In an HMBC experiment, the H3 methyl protons

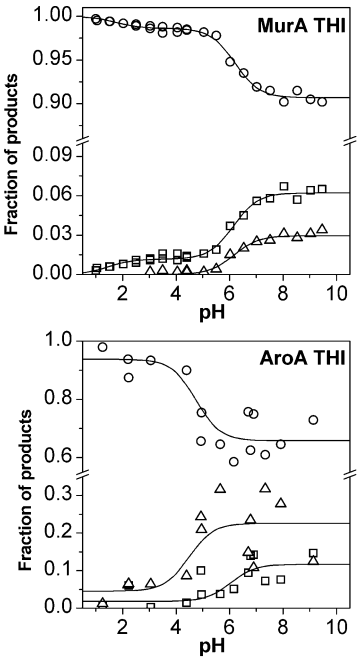

Figure 3. Product distributions for THI breakdown. For each compound, the proportion of the total products at each pH is plotted for (left) MurA THI and (right) AroA THI. (○) (UDP-GlcNAc or S3P) + pyruvate (**3**), (□) ketal (**4**), (△) EP-UDP-GlcNAc or EPSP (**5**).

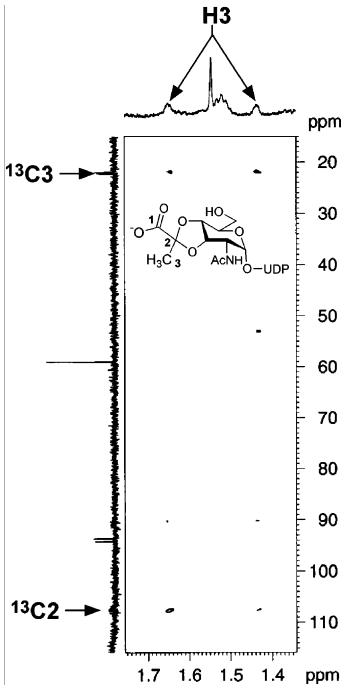

Figure 4. HMBC spectrum of ketal (**4**) from MurA THI. The spectrum was collected without ^{13}C decoupling, so the ^{13}C satellites of the methyl signal are observed in the ^1H spectrum.

were coupled to $^{13}C3$ ($\delta = 1.54$ ppm, $^1J_{C3-H3} = 128.2$ Hz). Cross-peaks were observed to $^{13}C2$ ($\delta = 107.8$ ppm) and $^{13}C3$ ($\delta = 22.0$ ppm, $^1J_{C2-C3} = 43.6$ Hz). These chemical shifts and coupling constants compare well with the reported values for the AroA ketal:[19] H3 ($\delta = 1.68$ ppm, $^1J_{C3-H3} = 128.5$ Hz); C2, 110.6 ppm; C3, 25.96 ppm. Very weak peaks indicating a possible correlation to $^{13}C1$ were observed at 176.5 ppm but were not clearly above the noise. Unidentified less intense peaks were observed near 53.3 and 90.2 ppm.

The only products of nonenzymatic breakdown detected by UV absorbance were UDP-GlcNAc, **4** and **5** (Figure 3). Breakdown of MurA [1-^{14}C]THI resulted in [1-^{14}C]pyruvate in the same proportion as UDP-GlcNAc, as well as **4** and **5**.

The product distribution was determined as a function of pH. At all pH's, the dominant products were {R−OH + pyruvate + Pi} (**3**), with the proportions of the ketal (**4**) and *enol*pyruvyl (**5**) products increasing with pH (Table 1, Figure 3). The proportion of UDP-GlcNAc decreased from 1 to 0.907, with pK_{a1} = 1.7 and pK_{a3} = 6.2. This agreed well with ketal (**4**) formation, which increased in proportion from 0 to 0.062 with pK_{a1} = 1.5 and pK_{a3} = 6.1. The proportion of EP-UDP-GlcNAc (**5**) also increased with pH from 0 to 0.030. There was no detectable **5** at pH < 3, but pK_{a3} = 6.2 was fitted, in good agreement with the pH dependence of **3** and **4** formation.

At pH 10, it is possible that a vanishingly small amount of [1-^{14}C]PEP was formed, ~0.4% of products. The amount formed was too small for the structure to be confirmed and could have arisen from cross-contamination during chromatography.

Breakdown Products: C−O versus P−O bond Cleavage. Pyruvate could arise from either C−O or P−O bond cleavage. To detect whether P−O cleavage occurred, MurA [^{33}P]THI was degraded in 50% (v/v) methanol, and the labeled products were separated by anion exchange chromatography. No monomethyl [^{33}P]phosphate was detected at pH 1, 8, 9, or 10. The limit of detection for P−O bond cleavage was estimated at 3% based on the molar fraction of methanol, 0.31, and amounts of [^{33}P]-phosphate detected.

The breakdown rate in 50% (v/v) methanol was 1.4×10^{-4} s^{-1} at pH 7.0 compared with 1.3×10^{-4} s^{-1} in buffer. The apparent product distribution changed, with a ratio **3**:**4**:**5** of 0.73: 0.24:0.02. The apparent increase in proportion of ketal to 0.24 was presumably due to a methyl ketal product coeluting with the intramolecular ketal product (**4**). The methyl ketal would be formed by methanol attack on the cationic intermediate. The proportion of *enol*pyruvyl product (**5**) was unchanged.

Breakdown Products: AroA THI. The products of AroA THI breakdown have been characterized previously.[14,19] In the present study, it appeared initially that there was no [1-^{14}C]-pyruvate formed at high pH, but extended incubation of authentic [1-^{14}C]pyruvate at high pH caused its HPLC retention time to shift from 13.0 to 8.2 min, presumably due to a condensation reaction.[24] At pH > 11, with reaction times of up to 3 weeks, the pyruvate peak was shifted completely to the 8.2 min peak. At pH 8−10, both peaks were detected, while, at lower pH's, only the pyruvate peak was detected. Taking this peak into account during THI breakdown gave correct mass balance for the reaction. As with the MurA THI, the dominant products were {R−OH + pyruvate + Pi} (**3**), with the proportions of the ketal (**4**) and EPSP (**5**) increasing with pH (Figure 3). The cause of the less reproducible product distribution data for AroA THI breakdown is not clear, though the fact that reactions had to be taken almost to completion in order to get enough ^{14}C counts in the small amounts of ketal (**4**) and EPSP (**5**) contributed.

Effect of Buffer on Product Distribution. The relatively large differences in the product distributions for MurA and AroA THIs (Figure 3) suggested that buffer conditions and/or other functional groups in the molecules affected the product distribution. For MurA THI, the ratio of products **3**:**4**:**5** was 0.91:0.06: 0.03 at pH > 7.5 in 50 mM bis(trispropane), Tris, or glycine. Adding 100 mM $Et_3NH{\cdot}HCO_3$ had no effect, with a **3**:**4**:**5** ratio of 0.90:0.07:0.03. However, with 60 mM $NH_4{\cdot}HCO_3$, the **3**:**4**:**5** ratio changed to 0.86:0.05:0.09 at pH 7.5, and 0.80:0.07:0.13 at pH 10.0. That is, the proportion of *enol*pyruvyl product increased, becoming greater than the ketal, which remained largely unchanged. The rate constant at pH 10.0 did not change, $k = 1.0 \times 10^{-6}$ s^{-1}. Thus the breakdown products of MurA THI were sensitive to the reaction conditions.

Discussion

Understanding which catalytic strategies an enzyme uses necessarily requires understanding which strategies are capable of working. Studying the nonenzymatic breakdown of the THIs of MurA and AroA lends insight into their reactivity, as well as the related compounds CMP-NeuAc (**1**) and CMP-deoxy-octonate (**2**). Studies on the THIs have been limited by their difficult syntheses and instability. By producing gram amounts of *E. coli* AroA and MurA and using them to synthesize THIs, we have been able to characterize the kinetics and products of THI breakdown over a pH range of 1−12.

Previously, it was shown that the MurA[13] and AroA[14] THIs were acid labile. The half-life of AroA THI was >48 h at pH 12. AroA THI yielded {S3P + pyruvate + Pi} (**3**) at low pH, with {ketal + Pi} (**4**) and {EPSP + Pi} (**5**) appearing at pH 7.[14] The dominant products of MurA THI degradation were {UDP-GlcNAc + pyruvate + Pi} (**3**). Our results agree with those findings. The rate constants of MurA and AroA THI degradation were similar to each other, within 15-fold at all pH's. The half-lives ranged from 1 s at pH 1 to 89 and 24 days at pH 12 for MurA and AroA THIs, respectively.

Mechanism of THI Breakdown. The proposed mechanism is described briefly here, followed by detailed discussions of specific parts. In the proposed mechanism, THI breakdown occurs by phosphate departure through a rate-limiting C−O bond cleavage that is intramolecular general acid catalyzed by the α-carboxyl group (Figure 5). The immediate product of C−O bond cleavage is proposed to be an ion pair complex[25,26] between an oxocarbenium ion, and phosphate, **6**−**8**. The dominant reaction at all pH's is addition of water, ultimately leading to **3**. As pH increases, the product distribution changes, with larger amounts of **4** and **5**. The product distribution is affected by the phosphate protonation state and the reaction conditions. The experimental results are discussed below in light of this proposed mechanism.

Evidence for C−O Bond Cleavage. The products **4** and **5** could only arise through C−O bond cleavage. However, {R−OH + pyruvate + Pi} (**3**) could arise through either C−O or P−O bond cleavage. MurA THI was degraded in the presence of 50% aqueous methanol at pH's 1−10 to detect any P−O bond cleavage. In the event of P−O bond cleavage, methanol would trap the metaphosphate intermediate (PO_3^-), forming monomethyl phosphate. The fraction of monomethyl phosphate formed is directly proportional to the mole fraction of methanol in the solvent when the reactant is monoanionic phosphate,[27,28]

(24) Margolis, S. A.; Coxon, B. *Anal. Chem.* **1986**, *58*, 2504.

(25) In the Winstein formalism,[26] ion pairs may be intimate or solvent separated. Our results do not allow us to make this distinction; therefore, we refer to them simply as ion pairs.

(26) Carey, F. A.; Sundberg, R. J. *Advanced Organic Chemistry*, 3rd ed.; Plenum Press: New York, 1990.

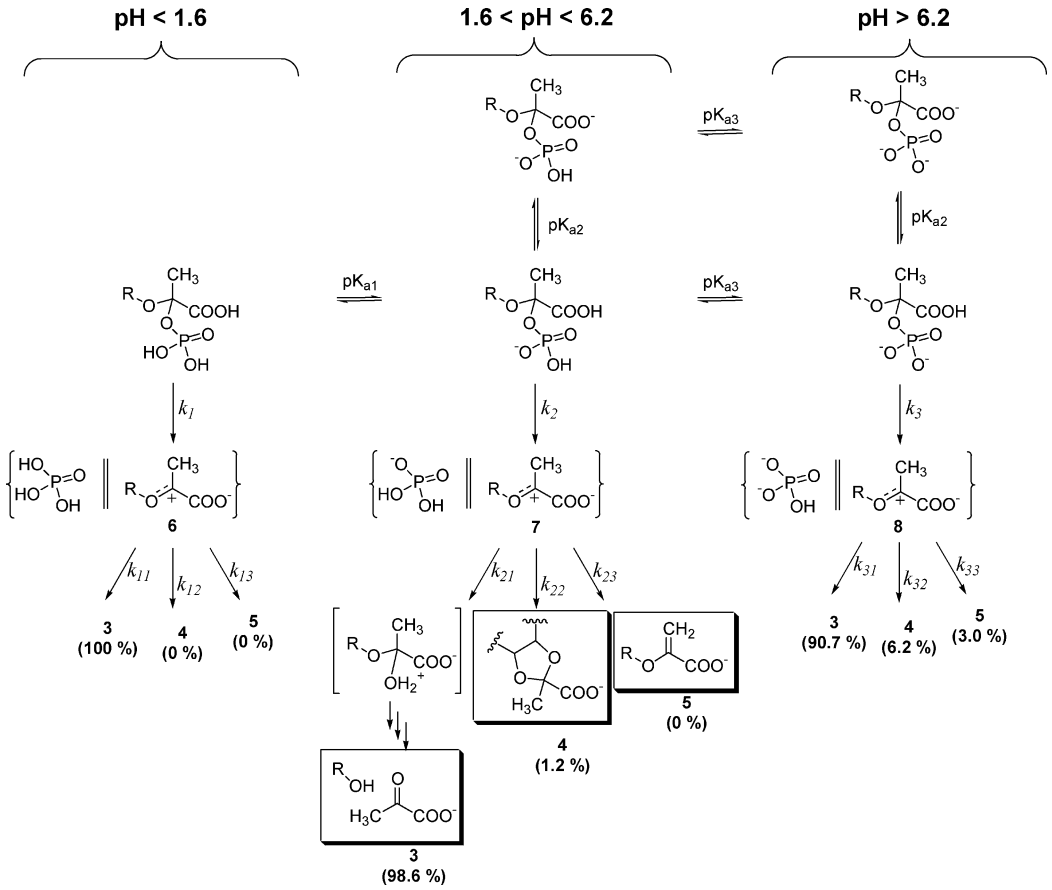

Figure 5. Reaction scheme for MurA THI breakdown. The proposed mechanism involves rate-limiting dissociation of phosphate (k_1, k_2, k_3) which is acid catalyzed by the α-carboxylic acid. The product distribution for MurA THI is shown. It depends on the fate of the initially formed oxocarbenium−phosphate ion pair complex (**6**−**8**). Increasing amounts of **4** and **5** at higher pH are attributed to increased ion pair lifetimes, allowing increasing amounts of nucleophilic addition by the adjacent hydroxyl to give **4** or deprotonation to give **5**. The product distribution for AroA THI is different (see text).

or in higher proportion when the reactant is dianionic phosphate.[27] There was no detectable monomethyl [^{33}P]phosphate formed from MurA [^{33}P]THI under any conditions. Levels of P−O bond cleavage at least as low as 3% would have been detected.

pH Dependence of Breakdown Rate. THI breakdown was acid catalyzed, with the pH dependence dominated by a ionizations with pK_{a2} = 3.2 (MurA) or 4.3 (AroA). Rates for MurA and AroA THIs were within a factor of 15 of each other at all pH's. The value of pK_{a2} for MurA THI was consistent with the combined electron withdrawing effects of a ketal oxygen and phosphate adjacent to the carboxylic acid. In comparison, the pK_a of the carboxylic acid of 2-phosphoglycolic acid is 3.6,[29] and that of the 2-cyclohexyloxyacetic acid is 3.5.[30] There was a weak dependence on an ionization with pK_{a4} = 8.8 in the MurA THI reaction, consistent with ionization of the uridine ring.[31] A negative charge on the uridine ring could electrostatically stabilize the proposed cationic intermediate. The reason for the higher apparent pK_{a2} = 4.3 for AroA THI was not clear but may have arisen from interaction with the triethylammonium ions present in the reaction mixture and/or the fact that there are more ionizable groups (the 1-carboxylic acid and 3-phosphate from the shikimate ring) nearby, raising pK_{a2} via through-space interactions.

Protonation of the THI phosphate had little or no effect on the rate. It would have taken a ≈3-fold change in rate to be observable in the pH-profile. The lack of effect on rate was unexpected; protonating the nonbridging oxygens of phosphate would have been expected to make it a better leaving group and therefore increase the rate. On the other hand, the lack of effect on protonation is consistent with the fact that the THIs have similar stabilities to the phosphodiester-containing **1** and **2**, as well as **9** and **10**.[32]

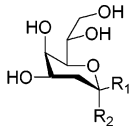

9: R_1 = O-$PO_3^=$, R_2 = COO^-
10: R_1 = COO^-, R_2 = O-$PO_3^=$

THI breakdown was insensitive to other changes in reaction conditions. The rate of MurA THI breakdown was unaffected by buffer conditions that changed the product distribution or by 50% methanol. The lack of effect with methanol was consistent with the previous observation of only a 2-fold

(27) Kirby, A. J.; Varvoglis, G. A. *J. Am. Chem. Soc.* **1967**, *89*, 415.
(28) Allen, C. M., Jr.; Jamieson, J. *J. Am. Chem. Soc.* **1971**, *93*, 1434.
(29) Hartman, F. C.; LaMuraglia, G. M.; Tomozawa, Y.; Wolfenden, R. *Biochemistry* **1975**, *14*, 5274.
(30) Charton, M. *J. Org. Chem.* **1964**, *29*, 1222.
(31) Privat, E. J.; Sowers, L. C. *Mutat. Res.* **1996**, *354*, 151.
(32) Liang, P.-H.; Lewis, J.; Anderson, K. S.; Kohen, A.; D'Souza, F. W.; Benenson, Y.; Baasov, T. *Biochemistry* **1998**, *37*, 16390.

decrease in the rate of CMP-NeuAc (**1**) breakdown in neutral 70% ethanol.[33]

Evidence for General Acid Catalysis. THI breakdown was acid catalyzed. The solvent deuterium KIE at pL 2.0 was 1.3 ± 0.4. This is typical of general acid catalysis previously observed with various acetal hydrolyses, 1.0−1.5,[29,34−36] and was similar to that for hydrolysis of **9** and **10** (1.1−1.2).[37] It was inconsistent with the inverse solvent deuterium KIEs observed for specific acid catalysis,[38] including 0.45 observed with CMP-NeuAc (**1**).[39] This is less than the solvent deuterium KIE for hydrolysis of the enol ether **11**,[40] ~5, which presumably reflects the larger intrinsic barrier to proton transfer involving C−H bonds compared with O−H···O in THI breakdown.

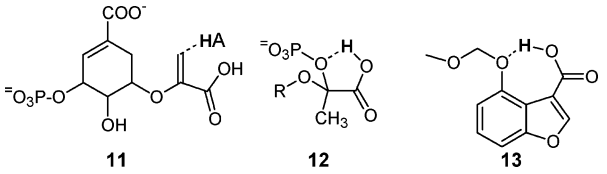

11 **12** **13**

If general acid catalysis is operative, the question becomes whether it is intramolecular catalysis by the α-carboxyl or the kinetically equivalent intermolecular catalysis by H_3O^+. With intramolecular general acid catalysis, proton transfer would be through a favorable five-membered ring structure (**12**). Kirby and co-workers showed that general acid catalysis of acetal hydrolysis with rate enhancements of almost 10^5 is possible even with a less favored seven-membered ring during proton transfer (**13**).[41,42]

For intermolecular general acid catalysis by H_3O^+, the pH dependence corresponding to pK_{a2} would correspond to the inductive effect of ionization of the α-carboxyl group. Carboxylate, COO^-, being electron donating relative to carboxylic acid, COOH, can better stabilize a cationic intermediate. This will lead to a decrease in rate upon α-carboxyl protonation, consistent with the rate profiles of the THIs. The most relevant analogues to help estimate the strength of the inductive effect would be the hydrolyses of **14**[43] and **15**,[34] where the cationic intermediate formed would be very similar to the THIs. The effect of carboxyl ionization was small in both cases, only 3-fold for **14** and 5-fold for **15**. In **15**, the reaction was reported to be general acid catalyzed by H_3O^+, so the α-carboxyl ionization effect was an inductive effect. Another example of inductive effects is **16**,[44] where ionization of the carboxyl group increased hydrolysis 90-fold. This was attributed to inductive effects because intramolecular general acid catalysis was not geometrically possible. Intramolecular general acid catalysis was proposed for hydrolyses of **17**[41] and **18**,[36] where 100- and 300-fold effects were observed.

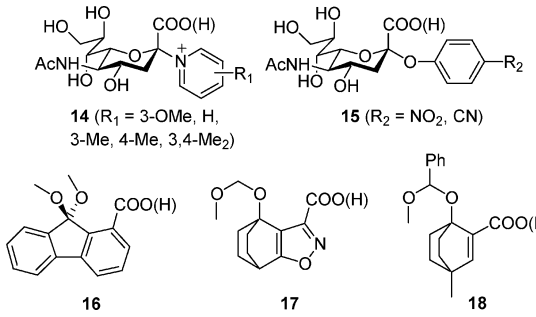

14 (R_1 = 3-OMe, H, 3-Me, 4-Me, 3,4-Me_2) **15** (R_2 = NO_2, CN)

16 **17** **18**

It is not possible to determine the exact magnitude of the effect of α-carboxyl ionization on THI breakdown because the pH profile was flat at the lowest pH's measured. However, based on the fact that the pH profile was flat for at least 1.5 (MurA) or 2.0 (AroA) pH units, the effect of carboxyl ionization was at least 30- to 100-fold. This is significantly larger than the inductive effects assigned to α-carboxyl ionization in **14** and **15**. On this basis, we propose that the general acid catalyst in THI breakdown is the intramolecular carboxyl group, rather than H_3O^+, though either alternative is possible. Regardless of the acid catalyst, the most important observation is that THI breakdown is catalyzed through protonation of the phosphate bridging oxygen rather than the nonbridging oxygens.

The THIs meet the conditions for general acid catalysis of acetals elucidated by Fife,[45] namely a good leaving group and a relatively stable oxocarbenium ion. They also meet the condition[38] that the pK_a of the proton acceptor, the bridging oxygen of the phosphate, changes dramatically between the reactant (~ −4) and phosphate product (1.8, 6.8, or 11.7),[46] with the pK_a of general acid catalyst, 3.2 (MurA) or 4.3 (AroA), between the two, except at pH < 1.6, where the product is H_3PO_4.

Product Distribution. The product distribution was affected by the identity of the THI (MurA versus AroA), pH, buffer and solvent composition. This implies that once the rate-limiting step had occurred, that is, cleavage of the C−O bond to form an ion pair complex (**6**−**8**), three distinct breakdown pathways were possible, all with relatively similar activation energies. This made the product distribution sensitive to reaction conditions. Water addition yields **3**; C3 deprotonation gives an overall phosphate elimination, yielding **5**, while nucleophilic attack by the adjacent hydroxyl yields **4**.

Without an ion pair complex, the oxocarbenium ion would undergo rapid water addition to yield only pyruvate (**3**). Oxocarbenium ions are highly reactive, with small intrinsic barriers to nucleophilic attack.[47] The oxocarbenium ions of sugars such as glucose are too reactive to have a finite lifetime in solution.[48] One of the more stable oxocarbenium ions found to date is from CMP-NeuAc (**19**), which had a lifetime in solution of $\geq 3 \times 10^{-11}$ s.[39] Its relatively high stability was attributed to the α-carboxyl group and the lack of an adjacent hydroxyl, features present in **6**−**8**.

Stabilization of the oxocarbenium ion in an ion pair complex makes formation of **4** and **5** possible. In the elimination reaction,

(33) Ruano, M.-J.; Cabezas, J. A.; Hueso, P. *Comp. Biochem. Physiol.* **1999**, *123B*, 301.
(34) Ashwell, M.; Guo, X.; Sinnott, M. L. *J. Am. Chem. Soc.* **1992**, *114*, 10158.
(35) Barber, S. E.; Dean, K. E. S.; Kirby, A. J. *Can. J. Chem.* **1999**, *77*, 792.
(36) Brown, C. J.; Kirby, A. J. *J. Chem. Soc., Perkin Trans. 2* **1997**, 1081.
(37) Baasov, T.; Kohen, A. *J. Am. Chem. Soc.* **1995**, *117*, 6165.
(38) Cordes, E. H.; Bull, H. G. *Chem. Rev.* **1974**, *74*, 581.
(39) Horenstein, B. A.; Bruner, M. *J. Am. Chem. Soc.* **1998**, *120*, 1357.
(40) Kresge, A. J.; Leibovitch, M.; Sikorski, J. A. *J. Am. Chem. Soc.* **1992**, *114*, 2618.
(41) Hartwell, E.; Hodgson, D. R. W.; Kirby, A. J. *J. Am. Chem. Soc.* **2000**, *122*, 9326.
(42) Dean, K. E. S.; Kirby, A. J. *J. Chem. Soc., Perkin Trans. 2* **2002**, 428.
(43) Chou, D. T. H.; Watson, J. N.; Scholte, A. A.; Borgford, T. J.; Bennet, A. J. *J. Am. Chem. Soc.* **2000**, *122*, 8357.
(44) Cherian, X. M.; Van Arman, S. A.; Czarnick, A. W. *J. Am. Chem. Soc.* **1990**, *112*, 4490.
(45) Fife, T. H. *Acc. Chem. Res.* **1972**, *5*, 264.
(46) Saha, A.; Saha, N.; Ji, L.-n.; Zhao, J.; Gregan, F.; Sajadi, S. A. A.; Song, B.; Sigel, H. *J. Biol. Inorg. Chem.* **1996**, *1*, 231.
(47) Richard, J. P.; Williams, K. B.; Amyes, T. L. *J. Am. Chem. Soc.* **1999**, *121*, 8403.
(48) Banait, N. S.; Jencks, W. P. *J. Am. Chem. Soc.* **1991**, *113*, 7951.

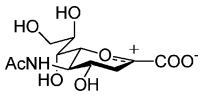

19

phosphate could act directly as a general base to deprotonate the C3 methyl or merely extend the lifetime of the oxocarbenium ion enough to allow some other group to act as a base. Although the methyl of the cationic intermediate is very acidic, $pK_a < 0$,[40] there is a significant kinetic barrier to C−H bond dissociation.[47] Elimination is slow compared to water addition with uncomplexed oxocarbenium ions, as illustrated by low rates and general base-catalyzed deprotonation of substituted 1-phenylethyl carbocations,[49] and with the oxocarbenium ion of acetophenone, where water addition was 19 000-fold faster than elimination,[47] though α-carbonyl substituents can have a large effect on product partitioning.[50,51]

There is no obvious role for phosphate in ketal formation beyond extending the lifetime of the oxocarbenium ion. Phosphate would be located on the opposite side of the electrophilic carbon from the nucleophilic hydroxyl, making general base catalysis difficult or impossible. At the same time, general base catalysis is likely unnecessary given the extremely high reactivity of the oxocarbenium ion.

MurA THI Product Distribution. With MurA THI, the proportions of **4** and **5** increased with pH. Two pK_a's controlled the product distribution, with $pK_{a1} = 1.6$ and $pK_{a3} = 6.2$. These were in the range expected for phosphate monoesters, 0.7−1.4 and 5.7−6.8,[29,46,52,53] though somewhat lower than observed with **9** and **10**, with $pK_{a3} = 6.8$ and 7.2, respectively.[32] Presumably the lifetime of the complex would increase as phosphate changed from neutral (**6**) to monoanion (**7**) to dianion (**8**) forms because of greater electrostatic interactions. The proportions of **4** and **5** would then show a pH dependency reflecting the pK_a's of the phosphate, precisely what was observed with MurA THI. The fact that these pK_a's did not affect breakdown rates supports the suggestion that the product distribution was determined *after* rate-limiting formation of **6**−**8**. This is further supported by the observation that (i) 60 mM $NH_4{\cdot}HCO_3$ in the MurA THI reaction mixture increased the proportion of **5**, without changing the proportion of **4** or the overall rate,[54] and (ii) reaction in 50% methanol caused no change in rate but increased the apparent proportion of ketal (**4**) to 0.24, presumably due to a methyl ketal product coeluting with **4**. The methyl ketal would be formed by methanol attack on the cationic intermediate.

The similarity of the pK_a's controlling **4** and **5** formation suggests that the role of phosphate may be the same in both, extending the lifetime of the ion pair complexes.

AroA THI Product Distribution. The pattern of **4** and **5** increasing with increasing pH also held with AroA THI, but the product distribution was less straightforward to interpret. The product distribution was reported previously with ratios **3**:**4**:**5** of 1:0:0 at pH 4 and 0.76:0.16:0.08 at pH 7.[14] In the present study, the product distribution also varied with pH, with ratios **3**:**4**:**5** of 0.90:0.02:0.09 at pH 4 and 0.66:0.11:0.23 at pH 7. That is, the elimination product EPSP (**5**) was formed in higher proportion than ketal (**4**). The reason for the difference in product distribution compared to both MurA THI and the previous report with AroA THI is not clear, but may be at least partly due to the reaction buffer. Reactions were conducted in the presence of ca. 100 mM triethylammonium ions, present from the anion exchange buffer. Triethylammonium ions interact specifically with AroA THI and/or EPSP, as evidenced by a differential shift in retention times, making separation possible, whereas these compounds coelute in other buffers.[14,17] The pK_a's affecting the product distribution were poorly defined but were ∼4.5 for EPSP (**5**) and 6.0 for the ketal (**4**). Clearly, the factors controlling the product distribution of AroA THI were different than those for MurA THI. The pK_a controlling **4** formation may have reflected the THI phosphate group, but the pK_a for **5** formation was inconsistent with a phosphate ionization. It was in the range expected for a carboxyl, but if intramolecular general acid catalysis by the α-carboxyl group is assumed, this group would always be a carboxylate in the ion pair complex, and there is no reason to expect an effect from the remote carboxyl of AroA THI.

Hydroxyl Departure. These experiments have been interpreted in terms of phosphate departure through C−O bond cleavage. The methods used in this study would not have directly detected hydroxyl (i.e., R−OH) departure, but all evidence points to it being a minor pathway. Hydroxyl departure would yield either {R−OH + PEP} or {R−OH + pyruvate + Pi} (**3**). PEP would be formed by deprotonating the C3 methyl of the cationic intermediate (**6**−**8**), giving an overall alcohol elimination. In MurA [1-^{14}C]THI breakdown at pH 10, a very small amount of [1-^{14}C]PEP may have been detected, ∼0.4% of the total products. This was very small compared to *enol*pyruvyl (**5**) formation, which also occurs through deprotonation of an oxocarbenium ion intermediate. Alternatively, **3** could be formed through either water addition to the cationic intermediate (**20**) or rapid P−O bond cleavage. The latter possibility was eliminated by the experiment with [^{33}P]THI.

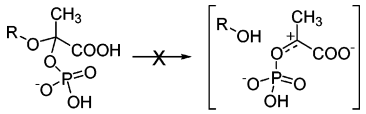

20

Based on their pK_a's, phosphate would be a better leaving group than R−OH at all pH's. This is consistent with the 7×10^6−fold higher rates of acid-catalyzed α-glucose 1-phosphate hydrolysis (extrapolated from ref 55) compared with α-methyl glucoside.[56] Our conclusions would be essentially unchanged if hydroxyl departure was a significant route of THI breakdown.

Other α-Carboxyketal Phosphates and Phosphodiesters. The α-carboxyketal phosphate functionality is rare. Cyclic α-carboxyketal phosphates **9** and **10** were synthesized as potential enzymatic intermediates of Kdo8P synthase.[32] Despite being acid labile and having lifetimes similar to the THIs, the

(49) Richard, J. P.; Jencks, W. P. *J. Am. Chem. Soc.* **1984**, *106*, 1373.
(50) Richard, J. P.; Lin, S. S.; Buccigross, J. M.; Amyes, T. L. *J. Am. Chem. Soc.* **1996**, *118*, 12603.
(51) Richard, J. P.; Amyes, T. L.; Lin, S. S.; O'Donoghue, A. C.; Toteva, M. M.; Tsuji, Y.; Williams, K. B. *Adv. Phys. Org. Chem.* **2000**, *35*, 67.
(52) O'Connor, J. V.; Barker, R. *Carbohydr. Res.* **1979**, *73*, 227.
(53) Massoud, S. S.; Sigel, H. *Inorg. Chem.* **1988**, *27*, 1447.
(54) Other buffers used in MurA THI breakdown could potentially have similarly affected the product distribution, but the smooth transitions between different buffers and the fact that different buffers at a given pH gave the same product distribution argue against this.
(55) Bunton, C. A.; Llewellyn, D. R.; Oldham, K. G.; Vernon, C. A. *J. Chem. Soc.* **1958**, 3588.
(56) Wolfenden, R.; Lu, X.; Young, G. *J. Am. Chem. Soc.* **1998**, *120*, 6814.

mechanism of breakdown was proposed to be different, with the pH dependence of degradation reported to be inconsistent with general acid catalysis by the α-carboxyl group.

There are two known α-carboxyketal phosphodiesters, CMP-NeuAc (**1**)[33,39,57,58] and CMP-deoxyoctonate (**2**).[59] These are acid labile and unstable at neutral pH, with half-lives at neutral pH of 12 and 0.6 h, respectively. The unusual reactivity of **2** was attributed to general acid catalysis combined with the hydroxyls at positions 4, 5, and 7 (or 8) enforcing ring conformations that are favorable for hydrolysis.[59] The weak pH dependence of hydrolysis at pH 7−8.5 and the large solvent deuterium KIE, 2.7, imply important differences from the THIs.[60]

The rates and products of THI breakdown were similar to those observed with CMP-NeuAc (**1**). Degradation was acid catalyzed, with pK_a = 4.7 (from Figure 2 of ref 57), and the product distribution changed with pH.[33,58,61] At pH 4, NeuAc (**21**, analogous to **3**) and CMP were the only products. The proportion of the elimination product (**22**, analogous to **5**) increased to 10% at pH 6,[58] 30% at pH 13, and 50% in anhydrous triethylamine.[61] A small amount of NeuAc 2-phosphate (**23**) was produced from concentrated aqueous base (30% NH_4OH or 50% triethylamine) or 100% triethylamine, indicating P−O5′ bond cleavage.

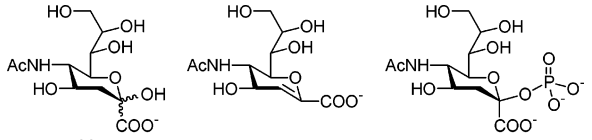

Role of α-Carboxyl Group. An α-carboxyl adjacent to the ketal phosphate is important for reactivity, as demonstrated by the fact that the acetal phosphate functionalities of sugar 1-phosphates and sugar nucleotide diphosphates (e.g., UDP-glucose) are not especially unstable. The half-life of α-glucose 1-phosphate is roughly 2 years at 25 °C and pH 7.[55]

Aside from its potential role as a general acid catalyst, the α-carboxyl would be expected to have a significant effect on THI stability based simply on steric effects. Acetals and ketals with secondary and tertiary substituents at R_1 (**24**),[62] and R_2 (**25**),[63] are more reactive and more prone to general acid catalysis

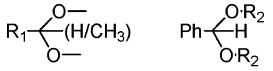

than those with less sterically demanding substituents. Although there are no close chemical analogues in the literature, it is reasonable to expect that part of the high reactivity of the THIs comes from the sterically demanding substituents, viz., a secondary alkoxy group (S3P or UDP-GlcNAc), a phosphate (sterically similar to R_2 = *t*-butyl), a methyl, and a carboxyl.

Relevance to the Enzymatic Breakdown of THIs. Nonenzymatic breakdown is proposed to proceed through an ion pair complex. In the enzymatic reactions, there is considerable circumstantial evidence for either cationic intermediates or cationic transition states in both formation and breakdown of the THIs.[8,10,19,64−66]

The dominant route of nonenzymatic THI breakdown was phosphate departure through C−O bond cleavage, the same bond that is broken in the forward enzymatic reaction. The results presented here show that protonating the bridging oxygen will be an effective catalytic strategy to promote phosphate departure. Presumably, protonating the ketal oxygen in the THI would promote R−OH departure. We recently proposed that the general acid catalyst in AroA for THI breakdown is Lys22,[17] located between the two potential leaving groups (**26**). According to the results presented here, it is ideally located to promote either phosphate or R−OH departure.

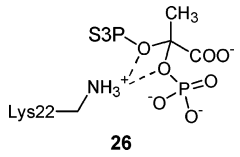

In the present study, THI breakdown at low pH was 14 000-fold (MurA) or 3000-fold (AroA) faster than that at pH 7.5. However, the specific activity of the Lys22Ala mutant of AroA decreased only 120-fold. Clearly, general acid catalysis is a relatively minor component of the 10^6-fold rate enhancement in enzymatic THI breakdown and much less than total catalytic advantage that could be achieved. Even if AroA took full advantage of the potential catalytic benefit of general acid catalysis, the rate, ∼1 s, would be less than k_{cat}, 56 s^{-1}.[67]

R−OH cleavage was a minor pathway in nonenzymatic breakdown, but in AroA-catalyzed THI breakdown there was only a 3:1 preference for phosphate departure over R−OH.[10,17] This implies that greater catalytic power is brought to bear on promoting R−OH departure to overcome its poorer inherent leaving group ability.

The products of the nonenzymatic reaction, predominantly **3**, were different from the enzymatic reaction, **5** (in the forward reaction). As shown in this study, the products of THI breakdown were altered relatively easily by reaction conditions. Thus, the main mechanistic imperative of AroA or MurA can be regarded as catalyzing C−O bond cleavage, with the products being determined by ensuring that the appropriate base is present to deprotonate C3 of the cationic intermediate (or cationic transition state) and shielding the cation from nucleophiles, particularly water.

Conclusions

Nonenzymatic breakdown of the THIs of the carboxyvinyl transferases MurA and AroA was examined. THI breakdown was through phosphate departure by C−O bond cleavage. The reaction was general acid catalyzed by protonation of the

(57) Comb, D. G.; Watson, D. R.; Roseman, S. *J. Biol. Chem.* **1966**, *241*, 5637.
(58) Horenstein, B. A.; Bruner, M. *J. Am. Chem. Soc.* **1996**, *118*, 10371.
(59) Lin, C. H.; Murray, B. W.; Ollmann, I. R.; Wong, C. H. *Biochemistry* **1997**, *36*, 780.
(60) Withers, S. G.; MacLennan, D. J.; Street, I. P. *Carbohydr. Res.* **1986**, *154*, 127.
(61) Beau, J. M.; Schauer, R.; Haverkamp, J.; Kamerling, J. P.; Dorland, L.; Vliegenthart, J. F. G. *Eur. J. Biochem.* **1984**, *140*, 203.
(62) Wiberg, K. B.; Squires, R. R. *J. Am. Chem. Soc.* **1981**, *103*, 4473.
(63) Belarmino, A. T. N.; Froehner, S.; Zanette, D.; Farah, J. P. S.; Bunton, C. A.; Romsted, L. S. *J. Org. Chem.* **2003**, *68*, 706.
(64) Anton, D. L.; Hedstrom, L.; Fish, S.; Abeles, R. H. *Biochemistry* **1983**, *22*, 5903.
(65) Bondinell, W. E.; Vnek, J.; Knowles, P. F.; Sprecher, M.; Sprinson, D. B. *J. Biol. Chem.* **1971**, *246*, 6191.
(66) Pansegrau, P. D.; Anderson, K. S.; Widlanski, T.; Ream, J. E.; Sammons, R. D.; Sikorski, J. A.; Knowles, J. R. *Tetrahedron Lett.* **1991**, *32*, 2589.
(67) Gruys, K. J.; Walker, M. C.; Sikorski, J. A. *Biochemistry* **1992**, *31*, 5534.

phosphate bridging oxygen, with rate constants controlled by ionizations with p$K_a = 3.2 \pm 0.1$ (MurA) or 4.3 ± 0.1 (AroA). The general acid catalyst was proposed to be the α-carboxyl group of the THI, although intermolecular general acid catalysis by H_3O^+ is also possible. The protonation state of the THI phosphate had no measurable effect on the rate, but it did affect the product distribution, with increasing the amounts of ketal and *enol*pyruvyl products at higher pH, with pK_a's of 1.6 and 6.2 for MurA THI.

These results are consistent with the observation in the AroA structure of a potential general acid catalyst of THI breakdown, Lys22, located such that it could protonate either the bridging oxygen of phosphate or the ketal oxygen. Protonating nonbridging oxygens in the THI phosphate is unlikely to be an effective catalytic strategy. The detailed chemical mechanisms of AroA and MurA are currently under investigation.

Acknowledgment. We thank Prof. Debra Dunaway-Mariano (University of New Mexico) for a generous gift of pyruvate phosphate dikinase and Dr. Don Hughes and Prof. Alex Bain (McMaster University) for invaluable assistance with the NMR analyses. We also thank the anonymous referees of this work for their valuable questions and comments. This work was supported by the Canadian Institutes of Health Research, as well as a graduate scholarship from the Natural Sciences and Engineering Research Council of Canada (B.B.).

JA0349655